Contact mechanics of real versus randomly rough surfaces: A Green's function molecular dynamics study

Carlos Campañá and Martin H. Müser

Department of Applied Mathematics, University of Western Ontario, London, ON, Canada N6A 5B7

PACS. 81.40.Pq – Friction, lubrication, and wear.
PACS. 46.55.+d – Tribology and mechanical contacts.

Abstract. – It is commonly assumed that knowing the height auto-correlation function of two solids in contact along with their materials properties is sufficient to predict the contact pressure distribution $P(p)$. We investigate this assumption with contact mechanics calculations that are based on quickly converging Green's function molecular dynamics. In our simulations, elastically deformable solids are pressed against a rigid substrate. Their profile is either given by experimental data or produced with random numbers such that the artificially generated height spectra ressemble that of the real profiles. Randomly rough surfaces produce Gaussian tails in the $P(p)$'s, while they are exponential for experimentally determined topographies. This difference, however, does not affect significantly the true contact area, which, for the given real profile is about 20% larger than that of the random surface. Both surfaces obey Persson's contact mechanics theory reasonably well.

Introduction. – Contact mechanics plays a crucial role in tribology. [1–4] For example, the amount of wear that occurs under sliding depends, among other variables, on the distribution of contact pressures. It has also been argued that Amontons' law, the linearity of static friction F_s and external load L, may often be the consequence of contact mechanics for the following reason: Due to most real surfaces having roughness on many different length scales, the pressure distribution in the real points of contact, $P(p)$, can remain surprisingly invariant over significant changes in L. [3, 6, 7] The main effect of increasing L would be to merely increase linearly the area of contact $A_{\rm real}$. Knowing or being able to predict $P(p)$ is also useful to determine the amount of plastic deformation, e.g., whenever the pressure p exceeds the hardness of the underlying material, one may expect plastic deformation to occur. Knowing pressure distributions may also be essential in predicting the friction coefficients and the thermal conductivity of an interface.

Sophisticated, theoretical models for contact mechanics are based on the assumption that roughness exists on many length scales [3,4,6–8]. Many times the focus is on self-affine topographies. This is because the height auto-correlation function of real surfaces, or more precisely, the height-difference correlation function $C_2(\Delta r)$ often increases algebraically according to:

$$C_2(\Delta r) \;=\; \Big\langle \{h(\mathbf{r}+\Delta\mathbf{r}) - h(\mathbf{r})\}^2 \Big\rangle$$

$$\propto \ \Delta r^{2H}. \tag{1}$$

Here, $h(\mathbf{r})$ is the height of a surface as a function of the in-plane vector $\mathbf{r} = (x, y)$, $\langle \ldots \rangle$ denotes a disorder average over the surface, H is called the Hurst roughness exponent ($0 < H < 1$), and Δr stands for the magnitude of the in-plane vector $\Delta\mathbf{r}$. The relation Eq. (1) typically holds for length scales Δr from about 1 nm up to 1 μm for highly polished surfaces and even further for regular surfaces. [3, 5] Higher-order correlation functions are commonly not considered to be relevant for contact mechanics. The surface topographies used in theoretical models are thus a choice of convenience. Sometimes, Weierstrass functions are used, which satisfy Eq. (1), or surface profiles are chosen at random, that is, they are chosen in such a way that the Fourier transforms $\tilde{h}(\mathbf{q}) = \tilde{h}^*(-\mathbf{q})$ of the height function $h(\mathbf{r})$ are independent Gaussian random variables with zero mean. Their second moments $\tilde{C}_2(\mathbf{q}, \mathbf{q}') = \langle \tilde{h}(\mathbf{q}) \tilde{h}^*(\mathbf{q}') \rangle$ obey: [9]

$$\tilde{C}_2(\mathbf{q}, \mathbf{q}') = h_\mathrm{s}^2 \, (q/q_\mathrm{s})^{2H+1} \, \Theta(q_\mathrm{s} - q) \, \Theta(q - q_\mathrm{l}) \, \delta(\mathbf{q} - \mathbf{q}'), \tag{2}$$

where $\Theta(\ldots)$ indicates the Heaviside step function which is unity for positive arguments and zero otherwise, and $\delta(\ldots)$ is the delta function. q_s and q_l are cutoffs in wave vectors at short and long wavelength, respectively, i.e., $q_\mathrm{l} \leq q \leq q_\mathrm{s}$, and h_s is the expected root mean square of the roughness associated with the short wavelength $\lambda_\mathrm{s} = 2\pi/q_\mathrm{s}$. It may be noted that the diagonal elements $\tilde{C}_2(\mathbf{q}, \mathbf{q})$ are proportional to the Fourier transforms of the real-space correlation function $C_2(\Delta r)$.

In the recent past, enormous strides have been made to predict the pressure distribution within contacts whose original surface profiles obey Eq. (1). The advances include a new analytical theory by Persson and coworkers, [3, 4, 6] who calculate the pressure distribution for elastic and elasto-plastic deformation in the case of both purely repulsive and adhesive interactions between the two solids. Moreover, new numerical multi-scale approaches were made by the same group [3, 6, 13] as well as by Robbins and coworkers. [7, 14, 15] Consensus has been reached on some issues, e.g., at small L, linear scaling of A_real with L is established for elastic, non-adhesive contacts. Both groups agree they are related via the root mean square of the surface slope or putting it mathematically [6, 7], A_real and L obey the equation

$$A_\mathrm{real} = \frac{\kappa}{\sqrt{\left\langle \{\nabla h(\mathbf{r})\}^2 \right\rangle}} \frac{L}{E'}, \tag{3}$$

where κ is a dimensionless proportionality coefficient. $E' = E/(1-\nu^2)$ is an effective modulus, E being Young's modulus and ν being the Poisson ratio. Disagreement persists as to whether κ depends on the roughness exponent H or whether it is constant. Persson predicts a value of $\kappa = \sqrt{8/\pi}$. Robbins and coworkers state values that are close to Persson's prediction for $H \approx 0.9$, while κ is close to $\sqrt{2\pi}$ for $H \approx 0.3$. This latter value corresponds to the one predicted by Bush *et al.*, [10] who based their calculations on a phenomenological, stochastic model in which asperities were described as paraboloid-shaped summits. There is also disagreement whether the tails of the pressure distributions are Gaussian as in the theory [6, 13] or exponential as found in simulations. [7]

Concerns have been raised that the numerical calculations were not converged to continuum mechanics, i.e., when only a small fraction of the area is in microscopic contact, fully converged calculations should obey the proportionality $P(p) \propto p$ at small values of p [4]. Also Hyun *et al.* argued that their observed linear decrease of κ with an increase in H may have been influenced by uncertainties in determining the true contact area. [7] Few simulations show the $P(p) \propto p$ feature, which leaves the determination of the nature of the pressure tails and also

the determination of the true contact area slightly ambiguous, as will be discussed in more detail in the model section. It is worth noting that Robbins' early method to discretise elastic objects was done such that roughness persisted down to the length scale of grid points (atoms). Such a procedure is certainly well motivated if one wants to know the distribution of forces on atoms. However, as we are interested in testing the solutions of continuum mechanics models, we shall try to mimic the continuum models as well as possible. This means that we will have to use discretisations that are smaller than the shortest wavelength on which roughness is found. It may be worth commenting that even the most advanced (and potentially accurate) Greenwood Williamson model based calculations [11] cannot be used to validate the correct value of κ, because any such treatment contains uncontrollable approximations.

In a recent paper by the present authors, it could be shown that Green's function molecular dynamics (GFMD) is an efficient tool to address contact mechanics of elastically deforming solids, [12], i.e., GFMD may be better suited to produce pressure distribution functions for static, elastic constants than the regular multi-scale approaches in which the three-dimensional solids are represented on ever more coarse-grained scales as one moves away from the interface. While some details of GFMD will be mentioned in the model section, we would like to refer to the original literature [12] for a detailed discussion.

The main purpose of this letter is to analyze the properties of well-converged pressure distributions in self-affine contacts that have the property displayed in Eqs. (1) and (2) by making use of GFMD. At the same time, we would like to investigate whether the contact mechanics of real surfaces resembles that of random surfaces. In particular, we would like to assess whether the pressure distributions for real surface topographies are similar to those of randomly rough surfaces.

Model and Methods. – In this study, we are concerned with the elastic, frictionless contact between two solids with self-affine surfaces. Use is made of the possibility to map such a system onto a model in which a flat elastically-deformable solid is pressed against a rigid, corrugated substrate. [2] The model thus consists of a rigid substrate, which can either have an experimentally determined topography or a numerically produced random height function $h(\mathbf{r})$. The other solid is a flat, discrete, elastic manifold, for which we chose both Lamé constant to be unity, which is equivalent to a Young's modulus of $E = 2.5$, a bulk modulus of $K = 5/3$, and a Poisson number of $\nu = 0.25$. In what follows, most stated quantities will be dimensionless, however, when pressure is not made dimensionless, then it will be stated in the unit of the Lamé constants.

Real surface topographies were obtained from atomic force microscopy (AFM) measurements of a highly-polished steel surface that had been subject to rubbing. [16] Before performing the measurements the surface material was turned and lapped under a cooling lubricant. The linear dimension of an AFM scan is $\mathcal{L} = 20\mu$m. Data points were available on a square grid with spacings of 10 nm. To reduce artifacts due to periodic boundary conditions, the experimental $h(\mathbf{r})$ data was corrected by terms linear and quadratic in x and y so that $h(\mathbf{r})$ became a continuous function at the boundaries. Between grid points, the height functions were interpolated with second-order polynomials such that first and second derivatives of $h(\mathbf{r})$ were continuous. The two-point correlation functions of our real surface can be characterized by a roughness exponent of $H = 0.84$ and cutoff $q_l = 10\,\mu m^{-1}$. The surfaces' root-mean slope, $\sqrt{\langle\{\partial h(x,y)/\partial x\}^2\rangle}$, was 0.1891.

Random surfaces with the same value of H were produced such that they had, on average, the same height power spectrum as that of the real surface. The random topographies were generated by using a Gaussian filter technique for the $\tilde{h}(\mathbf{q})$. [9] In those calculations, where we do not make a comparison between real and artificial surfaces, we reduced the root-mean

slope to 0.033. However, we kept the cutoff values in reciprocal space fixed and adjusted the parameter h_s in Eq. (2) for different values of H such that the root mean square slope remained constant.

The elastic manifold was simulated with GFMD. In a nutshell, GFMD only requires the simulation of an elastic sheet rather than that of a fully three-dimensional solid. The effective interactions between the atoms in the sheet, i.e., the elastic Green's functions, are chosen such that the sheet mimics the full solid. The full solid is a simple cubic solid with springs between nearest and next-nearest neighbors chosen such that a purely elastic medium is modeled, which is isotropic at long wavelengths. One of the main advantages of GFMD is that relatively few time steps are required for the elastic manifold to reach mechanical equilibrium. For more details on the methodology, we refer to our previously published model paper. [12]

Interactions between the two opposed surfaces are modeled with hard-wall potentials. If the z-coordinate of an atom belonging to the elastic slider at position (x, y) crosses through $h(x, y)$, the interaction energy increases from zero to infinity. The force that the hard-wall exerts on a surface atom (grid point) in the upper solid was obtained from the internal forces within the elastic manifold via a force balancing argument. As atoms are allowed to move transversally, we also have to determine the area that each atom occupies. This is done via a Voronoi construction. (For the surfaces investigated here, it turns out that the contact area would be overestimated by a little less than 2% if each atom in contact had been assigned a mean-field value for the contact area.)

Results. – The central quantity in this study is the pressure distribution in the contact. The full pressure distribution $P_f(p)$ consists of a δ-peak at $p = 0$, which is due to those areas that are not in contact and the distribution $P(p)$ averaged in the true contact points, i.e.,

$$P_f(p) = \frac{A_0 - A_{real}}{A_0} \cdot \delta(p) + \frac{A_{real}}{A_0} \cdot P(p), \tag{4}$$

where A_0 is the apparent or macroscopic surface area. For interactions with finite-range the delta peak will be broadened and it is not possible to define rigorously where contact exists. However, for hard-wall interactions use can be made of Eq. (4) to determine A_{real}, provided the histograms are converged, which is the case when $P(p)$ does not change (significantly) when the number of grid points in the elastic manifold is further increased. For small ratios A_{real}/A_0, a well-converged pressure histogram (in the sense of a continuum description) shows $P(p) \propto p$, which is also found in an individual Hertzian contact. For a more in depth discussion, we refer the reader to Refs. [3, 12, 14].

In Fig. 1, we compare the pressure distribution for real and ideal topographies for values of the load in which approximately 2% and 10% contact was established after equilibration. While the $P(p)$'s do not vanish completely in the limit $p \to 0$ at the employed discretisation of the elastic body ($N = 2048 \times 2048$), they are sufficiently well converged for the conclusions to be drawn in the subsequent paragraphs, as careful size analysis showed. The calculations are compared to the theory by Persson [6]. For this purpose, use was made of the analytical solution for the pressure distribution in the low-load limit, see Eq. (14) in Ref. [7].

The main difference between the graphs for artificially constructed and for real topographies is that the artificial surfaces produce Gaussian tails while the real topographies lead to exponential tails. This observation may settle the debate in the literature whether or not the distribution are Gaussian or exponential. Persson's theory predicts Gaussians, which is supported by our results for the Gaussian random surfaces, see also our previous results on *full* contact, [12] where the analytical solution for $P(p)$ in full contact [13, 17] was found to perfectly match our results. For the low-load limit, it was argued that exponential tails may be

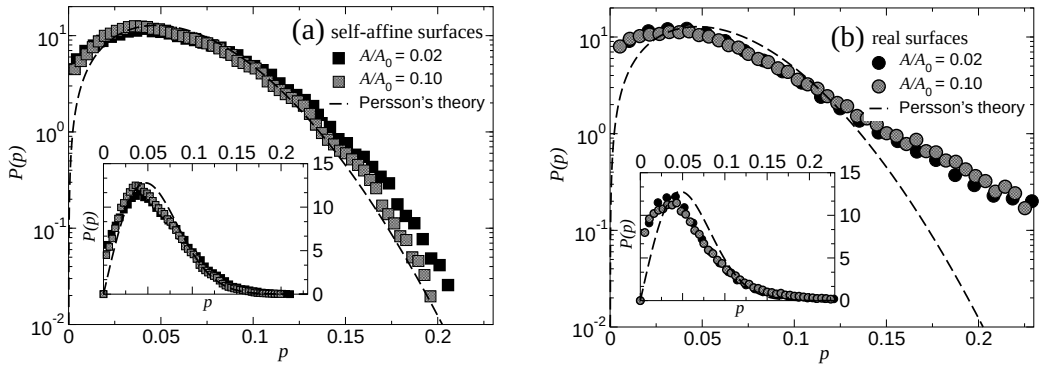

Fig. 1 – Pressure distribution $P(p)$ in the contact regions for (a) ideal and (b) real surfaces shown at two different relative contact areas A/A_0. Real and ideal topographies have similar two-point correlation functions $C_2(\Delta r)$. Black and grey symbols reflect roughly 2% and 10% relative contact area, respectively. The main graphs are lin-log plots and span the same domains in abscissa and ordinate. Insets are linear plots of the same data as in main figure. Comparison is made to Persson's contact mechanics theory.

the consequence of insufficiently converged calculations [4]. Indeed, we find that the $P(p)$ for artificial random surfaces look exponential as long as the grid spacing of the elastic manifold Δa is equal to or larger than the smallest wavelength λ_s on which roughness exists. Conversely, the $P(p)$ for real surfaces become even more clearly exponential when Δa is decreased below λ_s.

Once the $P(p)$'s are accumulated, it is possible to extract the true area of contact. Results are presented in Fig. 2, where the relative contact $A_{\rm real}/A_0$ is shown as a function of load. As observed in previous numerical studies [7, 13], linear behavior is found when the relative contact is less than roughly 10%. For the real contact topographies, the relative contact turns out to be about 20% larger than that of the ideally random surfaces. Despite this discrepancy, the pressure distributions for both types of surfaces remain rather invariant under a change of load that increases the relative contact from 2% to 10%.

The slightly increased contact area for real surfaces can be understood as follows: The worn-off asperities are less curved than the valleys. Since in small relative contact, the elastic manifold only samples the top of the asperities and not the valleys, greater contacts must be expected. Quantitatively, one can estimate the magnitude of the effect by comparing the root mean square slopes, i.e., $\langle(\nabla h)^2\rangle^{1/2}$, averaged over those areas where the curvature is negative to those averaged over positive surface curvature.

The slopes of the $A_{\rm real}(L)$ graphs at small L in Fig. 2 yield the dimensionless proportionality coefficient κ that relates the true contact area with the load. κ was introduced in Eq. (3). The results of our simulations are shown in Fig. 3. Three different values for the roughness exponent were considered, $H_1 = 0.2, H_2 = 0.5$, and $H_3 = 0.8$. It is found that for all three values of H, κ lies in between the predictions by Bush and Persson. Our results match those of Hyun *et al.* [7] reasonably well, although the change of κ with H is smaller

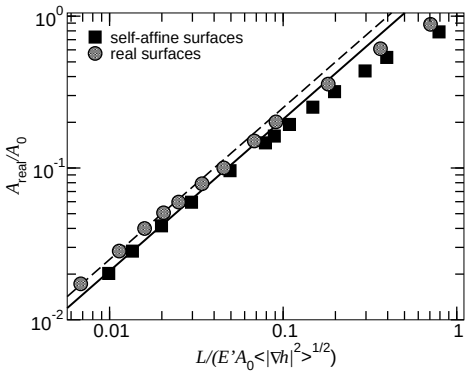

Fig. 2

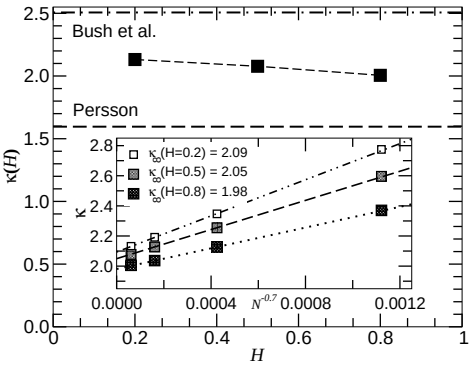

Fig. 3

Fig. 2 – Contact area ratio, A/A_0, versus applied load L. Linearity is observed for contact area ratios up to 10%. The discretisation of the elastic manifold is $N = 2048 \times 2048$ so that the discretisation is $\lambda_s/64$.

Fig. 3 – κ as a function of H. The values predicted by Bush *et al.* and Persson are plotted with dashed lines. Our results are represented with solid squares. Convergence with discretisation of the elastic manifold is analyzed in the inset.

in our work. However, the value of κ for $H = 0.5$ is very close to that recently stated by Hyun and Robbins [19]. The discrepancy between our and Hyun *et al.*'s previous result may be due to Hyun *et al.*'s former choice to keep the elastic manifold discrete at a length scale $2\pi/q_s$ and perhaps in part due to different choices for the Poisson ratio. Keeping surface roughness down to the discretisation of the elastic medium leads to a slight overestimation of A_{real} in particular at small values of H, where more roughness is on short length scales than for large H. It is yet interesting to note that extrapolation to rather accurate estimates for converged contact areas can be done at relatively moderate number of particles. We find that the leading-order corrections to the relative contact scale with $N^{-0.7}$ and that it appears to be possible to extrapolate to the continuum limit from data obtained with relatively moderate system sizes.

Conclusions. – In this work, we used our recently implemented GFMD technique [12] to study open questions evolving around the contact mechanics of elastic solids with self-affine surface roughness under the action of external loads. Special emphasis was given to the question how the pressure distributions and the true areas of contact differ between surfaces having either randomly self-affine or experimentally-measured topographies if their materials properties (that is, their elastic modulus) and their height power spectrum are identical.

Our results on the contact area of *randomly-rough* surfaces lie in between the predictions by Persson [3, 6] and those by Bush [10], which underestimate and overestimate the contact area by roughly 20%, respectively. Given that Persson's theory is less phenomenological than that of Bush and that generalizations, for instance to adhesion and dynamics, are more easily incoroporated, we have focused our attention to a comparison with Persson's theory, which predicts the functional form of the pressure distribution in a contact reasonably well.

While the net contact area of our artificial and the real surface are roughly similar, there

are qualitative differences in the tails of the distributions. We find that the ideally random surfaces produce Gaussian tails, while the real surfaces produce exponential tails. It is thus more likely to have very large pressures for surfaces with real topographies than for idealized random profiles. Yet, in both cases, it appears to be the case that the pressure distribution changes relatively little in the small load limit, in which the real area of contact grows linearly with the load. This observation supports the argument that contact mechanics of randomly rough surfaces can be hold responsible for Amontons' law [3], however, it does not rule out the argument that a constitutive law that relates normal and shear stress linearly can also lead to Amontons' law as argued in Ref. [20], in particular in those cases where surface profiles are not self-affine.

* * *

We are grateful for financial support from NSERC and discussions with Mark Robbins and Bo Persson. We would also like to thank D. Shakhvorostov for providing us with the experimental data.

REFERENCES

[1] Bowden F. P. and Tabor D., *Friction and lubrication* (Methuen, London; Wiley, New York) 1956
[2] Johnson K. L., *Contact Mechanics* (Cambridge University Press, New York) 1985
[3] Persson B. N. J., Albohr O., Tartaglino U., Volokitin A. I. and Tosatti E., *J. Phys.: Condens. Matter*, **17** (2005) R1
[4] Persson B. N. J., *Surf. Sci. Rep.*, **61** (2006) 201
[5] Koinkar V. N. and Bhushan B., *J. Appl. Phys.*, **81** (1997) 2472
[6] Persson B. N. J., *J. Chem. Phys.*, **115** (2001) 3840
[7] Hyun S., Pei L., Molinari J. F. and Robbins M. O., *Phys. Rev. E*, **70** (2004) 026117.
[8] Ciavarella M., Demelio G. and Murolo C., *J. Strain Analysis*, **40** (2005) 463
[9] Meakin P., *Fractals, scaling and growth far from equilibrium* (Cambridge University Press, New York) 1997
[10] Bush A. W., Gibson R. D. and Thomas T. R., *Wear*, **35** (1975) 87
[11] Ciavarella M.,Delfine V. and Demelio, *J. Mech. Phys. Solids*, (2006) doi:10.1016/j.jmps.2006.05.006
[12] Campañá C. and Müser M. H., *Phys. Rev. B*, **74** (2006) 075420
[13] Yang C., Tartaglino U. and Persson B. N. J., *Eur. Phys. J. E*, **19** (2006) 47.
[14] Luan B. Q. and Robbins M. O., *Nature*, **435** (2005) 929.
[15] Pei L., Hyun S., Molinari J. F. and Robbins M. O., *J. Mech. Phys. Solids*, **53** (2005) 2385
[16] Dmitry Shakhvorostov, , (private communication)
[17] Greenwood J. A., *P I Mech. Eng. J-J. Eng.*, **210** (1996) 281
[18] Pei L., Hyun S., Molinari J. F. and Robbins M. O., *J. Mech. Phys. Solids*, **53** (2005) 2385
[19] Hyun S. and Robbins M. O., *Tribol. Int.*, (submitted)
[20] Müser M. H., Wenning L. and Robbins M. O., *Phys. Rev. Lett.*, **86** (2001) 1295